ANNUAL REPORT 2005

Independent tests of vector-valued probabilistic seismic hazard: precariously balanced rocks in southern California

Matthew Purvance[1], James Brune[1], Rasool Anooshehpoor[1], Hong Kie Thio[2], and Paul Somerville[2]

[1]Seismological Laboratory, University of Nevada, Reno
[2]URS Corporation

INTRODUCTION

Recently Purvance et al. (2004) developed a methodology to use precariously balanced rocks (PBRs) to test the output of probabilistic seismic hazard analyses (PSHA). This is accomplished by convolving the PBR fragility surface (Figure 1a) with the vector-valued PSHA (Figure 1b), resulting in the vector-valued overturning rate (Figure 1c). Summing this rate over all ground motions produces the total overturning rate; a Poissonian recurrence assumption results in the PBR failure curve (Figure 1d). The number of years required for overturning with a 95% probability, denoted as T_{95}, is subsequently compared with the PBR ages for consistency. Bell et al. (1998) found that some PBRs in the Mojave Desert are at least 10 ka; this will be used subsequently as a proxy for the PBR ages. Such a comparison has been applied to PBRs near the Mojave section San Andreas fault (Region 1), between the San Jacinto and Elsinore faults (Region 2), and near the White Wolf fault (Region 3) (see Figure 2). Furthermore vector-valued PSHA estimates that utilize the ground motion prediction equations of Abrahamson and Silva (1997) (AS97) and the new NGA equations of Abrahamson (2005) (A05) will be compared against the 10 ka PBR age. These ground motion prediction equations utilize similar functional forms while the A05 model includes recent data from the Chi-Chi, Duzce, Izmit, and Denali earthquakes.

REGION 1

The seismic hazard in Region 1 is dominated by M=8 earthquakes at distances less than ~ 30 km. Background seismicity has been excluded from the ground motion models. Figure 3a shows that the Region 1 T_{95} values are generally less than 10 ka for ground motion models that utilize the AS97 prediction equations. Thus the PBRs at these sites would have overturned with a 95% probability in less than the presumed PBR age. As a result the existences of these PBRs are inconsistent with the ground motion models that utilize the prediction equations of AS97. The T_{95} values derived from the ground motion models that use the A05 prediction equations (Figure 3b) are generally greater

than 10 ka. Hence the PBRs require greater than 10 ka to overturn with a 95% probability and are therefore deemed consistent with the ground motion models.

REGION 2

The Region 2 PBRs are located southeast of the Region 1 sites (Figure 2) where the hazard is dominated by M=7 earthquakes on the San Jacinto and Elsinore faults. The T_{95} values for Region 2 PBRs are shown in Figure 4a (Figure 4b) for the ground motion models that utilize the prediction equations of AS97 (A05). The PBRs are numbered by the convention shown in Figure 2. Again, the PBRs are generally inconsistent with the ground motion models based on the prediction equations of AS97 and consistent with those that use the A05 prediction equations. These sites span greater than 100 km parallel to the San Jacinto and Elsinore faults.

REGION 3

PBRs in Region 3 lie very near to the White Wolf fault, the source of the M=7.7 1952 Kern County earthquake. Rupture directivity resulted in overturned transformers over a large region as documented by Peers (1955). Brune et al. (2004) found PBRs within a kilometer of the fault on the footwall side north of the region where transformers overturned. On the hanging wall side, though, PBRs and semi-PBRs are found at distances greater than approximately 9 km from the fault trace. Brune et al. (2004) argue that the asymmetry in ground motion resulting from the thrust faulting geometry has augmented the distribution of PBRs in Region 3. The T_{95} values are shown in Figure 5 where the footwall sites have been designated as site 1 and the hanging wall sites have been designated as site 2. The PBRs are generally consistent with ground motion models that utilize the A05 prediction equations (Figure 5b). The footwall PBRs are inconsistent with ground motion models that utilize the AS97 prediction equations, though (Figure 5a).

INVERSE STUDY

As the size and shape of a slender block changes, the resulting overturning rate changes in a systematic way. Hence it is possible to predict the geometrical attributes of blocks that will overturn with a specified probability over a specified time interval. Figure 6a shows the locations of sites along a transect of the San Andreas fault for which the vector-valued PSHA have been calculated. Hard rock conditions have been assumed at each site. Figure 6b shows the height-to-width ratios of ~ 1 m tall blocks that overturn with 95% probability in 10 ka along this transect when exposed to ground motion models based on the prediction equations of AS97 (red line) and A05 (blue line). Ground motion models that use the AS97 prediction equations result in blocks that overturn with a 95% probability with significantly larger height-to-width ratios in 10 ka; these results highlight the significant reduction in ground motions achieved in A05 when compared against AS97.

These results can be used in order to predict overturning as a function of time for man-made objects. For instance, Figure 7 shows the failure surfaces for unrestrained hot water heaters at the sites shown in Figure 6a. These results may be very useful for loss estimation in urban areas resulting from seismic hazard models.

DISCUSSION

These research initiatives mark an important step towards utilizing PBRs to both test ground motion models and carry out loss estimation. As shown above, ground motion models based on the prediction equations of AS97 are generally inconsistent with PBRs, while those based on the prediction equations of A05 are more consistent with PBRs. These are important findings that suggest the new ground motions added in A05 may be representative of typical ground motions for these distances and magnitudes. Future PBR initiatives will utilize the fact that several PBRs exist at a particular site and may act to lower the constraint provided by PBRs. The loss estimation provided herein assumes hard rock site conditions. Future loss estimations will rely heavily on site-specific PSHA initiatives.

REFERENCES

Abrahamson, N.A. and W.J. Silva (1997). Empirical response spectral attenuation relations for shallow crustal earthquakes, *Seism. Res. Lett.* **68** (1), 94-127.

Abrahamson, N.A. (April 1, 2005 *personal comm*.). Preliminary model of the Abrahamson and Silva (1997) attenuation relations from the Next Generation Attenuation project.

Bell, J.W, J.N. Brune, T. Liu, M. Zreda, and J.C. Yount (1998). Dating precariously balanced rocks in seismically active parts of California and Nevada, *Geology* **26** (2), 495-498.

Brune, J.N., A. Anooshehpoor, B. Shi, and Y. Zeng (2004). Precarious rock and overturned transformer evidence for ground shaking in the M_s 7.7 Kern County earthquake: an analog for disastrous shaking from a major thrust fault in the Los Angeles basin, *Bull. Seism. Soc. Am.* **74** (6), 1993-2003.

Peers, G.A. (1955). Damage to electrical equipment caused by the Arvin-Tehachapi earthquake, in *Bulletin 171 of the California Division of Mines*, G.B. Oakeshott (editor), 237-248.

Purvance, M.D., J.N. Brune, A. Anooshehpoor, H.K. Thio, and P. Somerville (2004). Precariously balanced rock toppling constraints and vector-values hazard, *Proceedings 2004 SCEC Conference*, Palm Springs, Ca., Sept. 20-22.

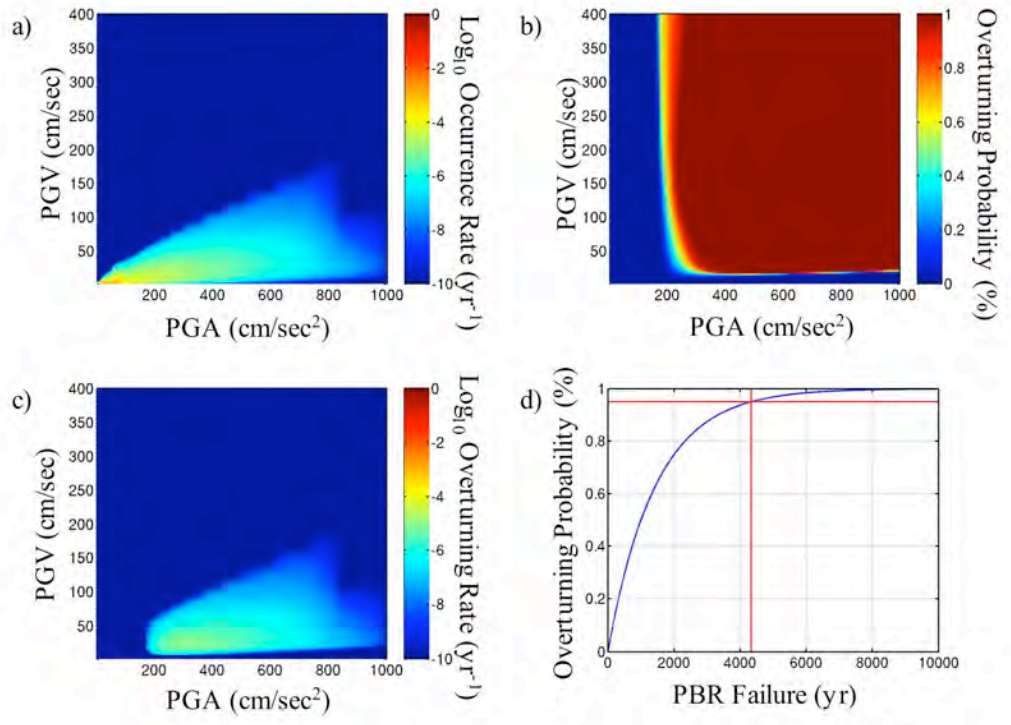

Figure 1 – Depiction of the process of obtaining a PBR constraint. The vector-valued PSHA (a) is multiplied by the PBR fragility surface (b), yielding the vector-valued overturning rate (c). A Poissonian assumption results in the failure curve (d). The T_{95} value is taken as the time required for overturning with the 95% probability (red lines).

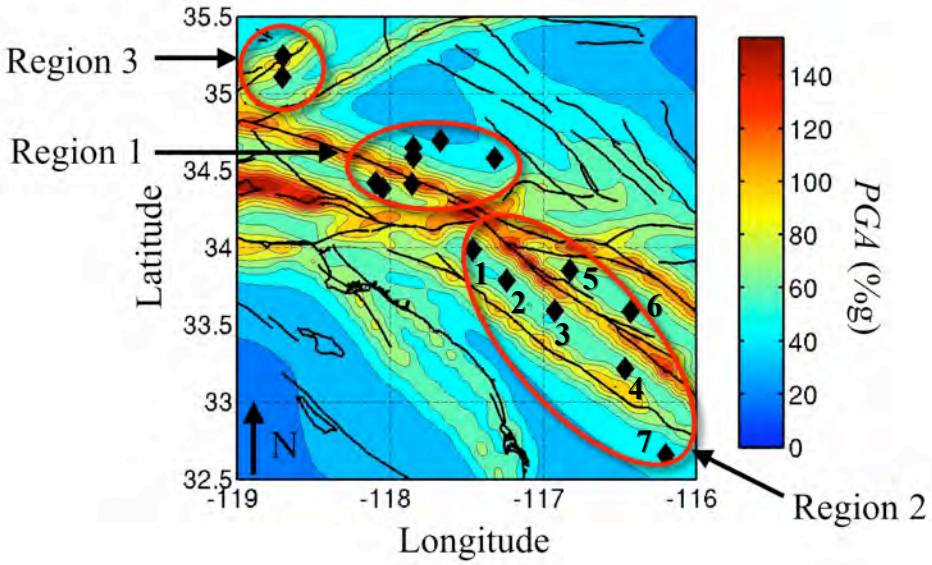

Figure 2 – 2002 National Seismic Hazard Map for the 2% probability of exceedence in 50 years for PGA overlain by the CGS fault database and PBR sites. Region 1 includes PBR sites along the Mojave section of the San Andreas fault, Region 2 includes PBR sites between the San Jacinto and Elsinore faults, and Region 3 includes PBR sites near the White Wolf fault.

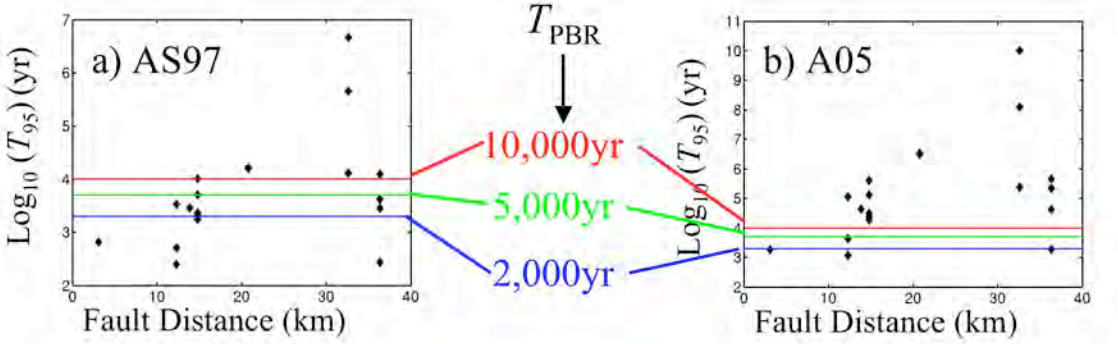

Figure 3 – Comparison between the Region 1 T_{95} values for ground motion models that utilize the prediction equations of a) Abrahamson and Silva (1997) and b) Abrahamson (2005). The 2 ka, 5 ka, and 10 ka contours are shown for comparison. The constraints are plotted with increasing distance from the San Andreas fault.

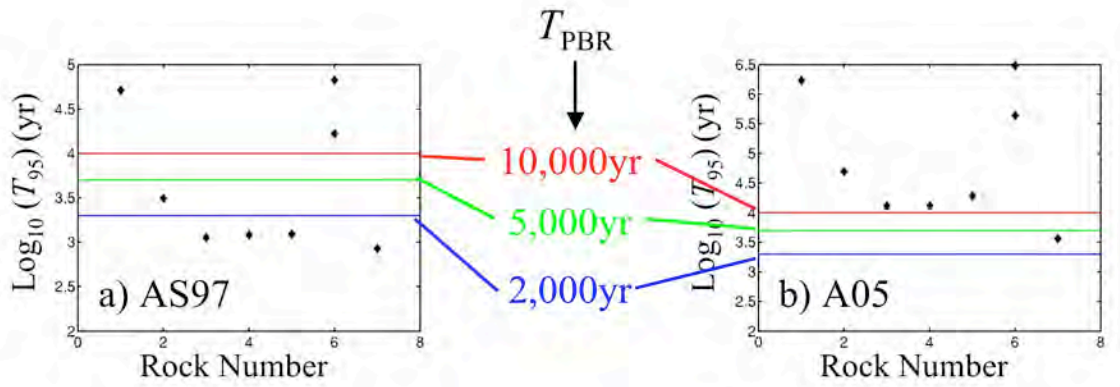

Figure 4 – Comparison between the Region 2 T_{95} values for ground motion models that utilize the prediction equations of a) Abrahamson and Silva (1997) and b) Abrahamson (2005). The 2 ka, 5 ka, and 10 ka contours are shown for comparison. The constraints are numbered as shown in Figure 2.

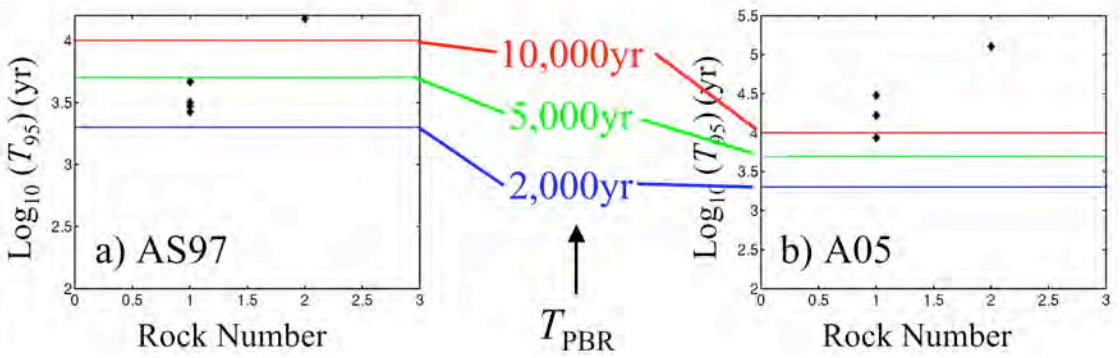

Figure 5 – Comparison between the Region 3 T_{95} values for ground motion models that utilize the prediction equations of a) Abrahamson and Silva (1997) and b) Abrahamson (2005). The 2 ka, 5 ka, and 10 ka contours are shown for comparison.

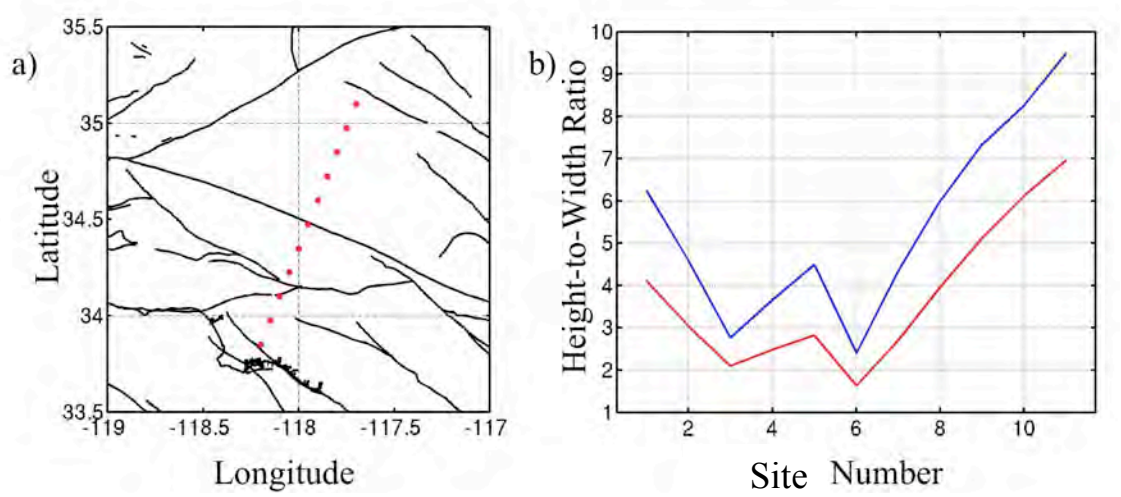

Figure 6 – a) Location of sites along a transect of the San Andreas fault used as an example of the inversion initiative. b) Height-to-width ratio of slender blocks that overturn with 95% probability in 10 ka based on the ground motion prediction equations of AS97 (red) and A05 (blue).

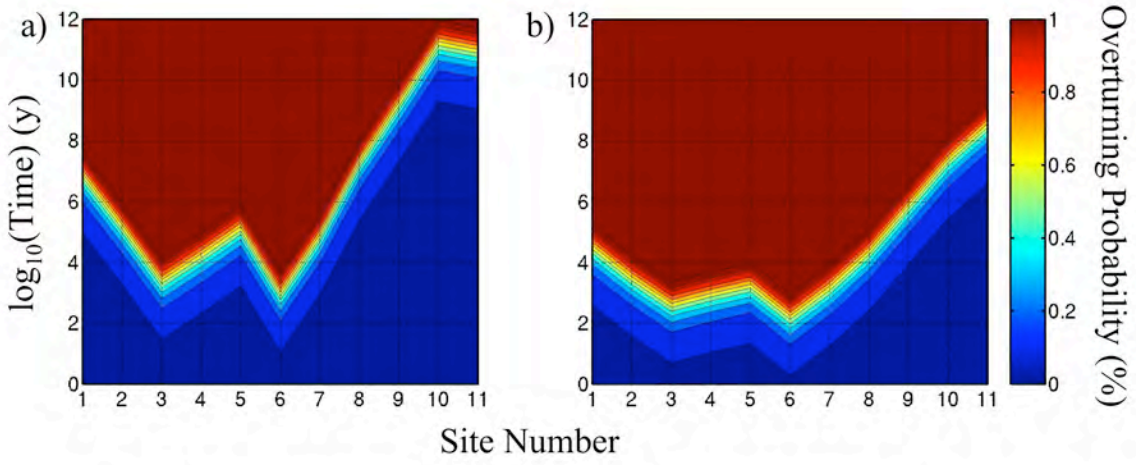

Figure 7 – Overturning probability for water heaters located at the sites shown in Figure 6a for ground motion models that utilize the prediction equations of AS97 (a) and A05 (b) as a function of time.